Theory of the optical properties of resonant states in nitrogen-doped semiconductor alloys*

Massimo Altarelli
Department of Physics, University of Illinois at Urbana-Champaign, Urbana, Illinois 61801
(Received 3 February 1975)

The optical properties of N-doped semiconductor alloys, such as GaAs-P and In-GaP, are investigated theoretically in the range of compositions, near the direct-indirect crossover, in which the discrete electronic state associated with the nitrogen trap is degenerate with the conduction-band continuum near the center of the Brillouin zone. The resolvent-operator formalism is applied to obtain the density of states and the optical absorption and emission spectra, by approximating the short-range impurity potential by a Koster-Slater interaction and using a simple parametrized description of the density of states of the host alloy. The presence of the discrete autoionizing trap state is shown to produce a characteristic Fano resonance-antiresonance line shape, in agreement with recent experimental observations, and in contrast to earlier theoretical predicitons of a sharp and resonantly enhanced emission spectrum.

I. INTRODUCTION

The dramatic influence of isoelectronic impurities[1] on the luminescence properties of semiconductors has been the object of extensive investigation since the discovery[2,3] of the nitrogen trap in GaP. In recent years, the effect of the N trap on the luminescence of ternary alloys, such as[4-6] $GaAs_{1-x}P_x$ and[7,8] $In_{1-x}Ga_xP$, which can be prepared in the whole range of compositions, and whose lowest band gap is direct or indirect if x is smaller or larger than a critical value x_c, has also been investigated. The possibility of a continuous variation of the band structure of the host alloy, besides being of great importance in optimizing the efficiency of light-emitting devices,[9] has led to the interesting experimental observation of resonant impurity states.[6,7] In fact, the discrete electronic state introduced by the N trap, and giving rise to the A-line emission, is mostly associated with the conduction-band minimum at the X point of the Brillouin zone, even when the absolute minimum is at Γ, i.e., for $x < x_c$. In this case, the discrete level is degenerate with the band continuum near the center of the zone, and is autoionizing, due to the large crystal-momentum components of the impurity potential.

The existence of resonant impurity states, predicted by the standard scattering theory applied to solids,[10,11] has been discussed theoretically for these systems[6,7,12] in terms of a realistic model, based on a parametrized description of the host-alloy density of states and on a one-band one-site Koster-Slater form for the nitrogen potential. This model has met a remarkable success in predicting the existence and location of the resonant state, as well as in accounting for the behavior of recombination processes in the range of compositions in which the N trap produces a *bona fide* bound state.[9,13,14]

The optical properties in the range of composition in which the impurity introduces a resonant state in the band continuum are more intriguing. The experience of similar situations in atomic[15] and solid state physics[16,17] suggests that the interference of transitions to the discrete level and to the continuum in which it is embedded shall result in an asymmetric Fano absorption (or emission) line shape, rather than in a sharp and very intense structure, as predicted by previous calculations.[7,12] Recent experimental observations for $GaAs_{1-x}P_x$:N provide indeed no evidence of the predicted emission enhancement as the energy of the resonant state is very close to the conduction-band minimum[18] and show an emission profile as well as an effective index of refraction dispersion in agreement with the Fano interference mechanism.[19]

The purpose of the present paper is to derive a comprehensive theory and carry out extensive calculations of the optical properties of the resonant states of the N impurity in the band continuum of semiconductor alloys. We will adopt the simple but realistic Koster-Slater description of the impurity potential and the parametrization of the host density of states introduced in Ref. 6 and successfully applied to the investigation of bound states. It will be most convenient to formulate the problem of resonant states and of their optical properties in the Green's-function or resolvent-operator formalism,[20,21] in which the quantities of interest here, such as densities of states, spectral functions, etc., have very simple formal expressions. It will be shown that the presence of the resonant state greatly modifies the continuum line shape, redistributing the oscillator strength in such a way as to produce a broad enhancement on the low-energy side of the resonance and a sharper dip (antiresonance) on the high-energy one. These qualita-

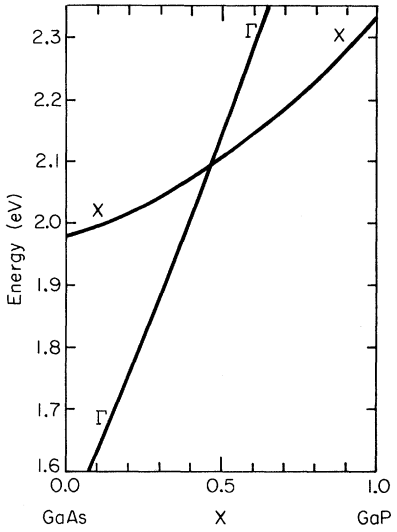

FIG. 1. Energy (in eV) of the conduction-band minima, with respect to the top of the valance band, in $GaAs_{1-x}P_x$, as a function of composition.

tive features of the oscillator strength are essentially unchanged by including the electron-hole Coulomb interaction in the calculation, and are in good agreement with effective-index data[18,19] for $GaAs_{1-x}P_x$.

The paper is organized as follows. In Sec. II we briefly recall, for convenience of the reader, the main features of the realistic model adopted and the expressions of the quantities of interest here in the resolvent-operator formalism. In Sec. III, we will derive and compute expressions for the density of states; the spectral weight of the region near Γ in the Brillouin zone; and the shape of the optical absorption and emission spectra, neglecting completely excitonic effects, i.e., considering transitions from resonant electrons to free holes. The electron-hole interaction is approximately included in the model in Sec. IV, and is shown to produce a considerable sharpening of the optical spectra, but without changing the qualitative features of the line shape. Finally, in Sec. V, the results obtained will be summarized, discussed, and compared to the available experimental data.

II. BASIC FORMALISM AND APPROXIMATIONS

Let us now briefly recall the parametrized description[6,7] of the electronic structure of the host alloys which will be used in the following. In Figs. 1 and 2 the energies (with respect to the top of the valence band) of the relevant conduction-band minima are shown as a function of alloy composition, for $GaAs_{1-x}P_x$ and $In_{1-x}Ga_xP$, respectively.[22,23] As it is well known, this dependence of the band gaps on composition x is well reproduced by a simple quadratic function of the form

$$E_i(x) = a + bx + cx(x-1). \tag{1}$$

Following the scheme proposed in Refs. 6 and 7, we will describe the conduction-band density of states by dividing the Brillouin zone into three regions, containing the Γ, the L and the X minima, respectively, and associating to each of them a density of states of the form

$$\rho_{0i}(E) = C_i(E - E_i)^{1/2}(E_i + 2\Delta_i - E)^{1/2}, \tag{2}$$

where the width $2\Delta_i$ is determined by fitting pseudopotential calculations with linearly interpolated form factors,[6,7] and the parameter C_i is chosen so that

$$\int_{E_i}^{E_i+2\Delta E_i} \rho_{0i}(E)\,dE \equiv \tfrac{1}{2}\pi C_i \Delta_i^2 \tag{3}$$

equals the contribution of the ith zone, as obtained from the pseudopotential calculation, to the integrated density of states normalized to one electron per spin. In $GaAs_xP_{1-x}$, the region surrounding L does not play an important role, as the gap at L is

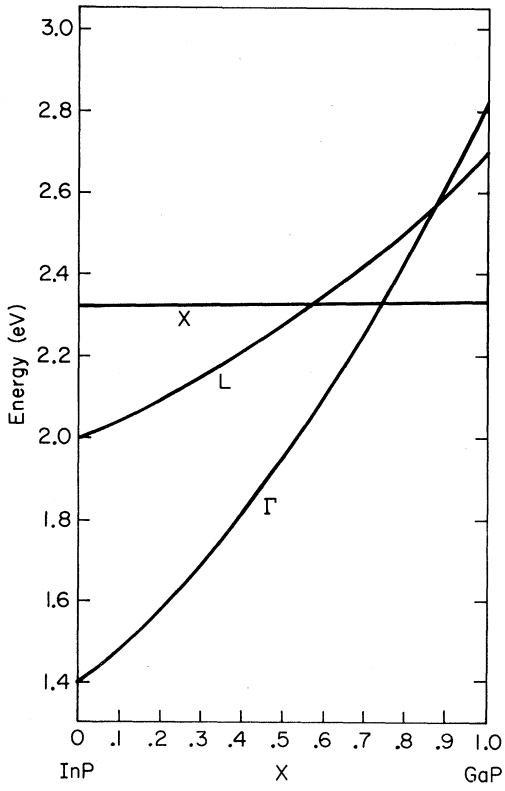

FIG. 2. Energy (in eV) of the conduction-band minima, with respect to the top of the valence band, in $In_{1-x}Ga_xP$, as a function of composition.

always larger than at X and, for the purposes of this calculation, the two corresponding regions can be merged into one. In $In_{1-x}Ga_xP$, on the other hand, the L minimum crosses both Γ and X and one must therefore retain the three regions. The parameters C_i and Δ_i are assumed independent of x and are computed at values of x near the direct-indirect crossover. The variation of the density of states with composition is then obtained by including the dependence of E_i on x, Eq. (1), in Eq. (2).

The nitrogen impurity potential is described by an attractive one-site Koster-Slater potential V, acting on electrons in the conduction band, and completely specified by one parameter, V_0 (<0), given by

$$\langle \vec{R}|V|\vec{R}'\rangle = V_0\delta_{\vec{R}\vec{0}}\delta_{\vec{R}'\vec{0}}, \tag{4}$$

where $|\vec{R}\rangle$ is the conduction-band Wannier function of the site $\vec{R}$, and the impurity is located on the origin $\vec{0}$. In the Bloch representation, Eq. (4) corresponds to a constant matrix element

$$\langle \vec{k}|V|\vec{k}'\rangle = U_0 \equiv V_0/N, \tag{5}$$

where $|\vec{k}\rangle$ and $|\vec{k}'\rangle$ are normalized Bloch states in the conduction band and N is the number of unit cells. The value of V_0 is chosen empirically[6,7] by fitting the experimental electron binding energy E_b in GaP:N, given in the Koster-Slater model by the equation

$$V_0 \int \frac{\rho_0(E')}{E_X - E_b - E'}\, dE' = 1. \tag{6}$$

It was shown[6,7] that, in this simple but realistic model, for compositions slightly below x_c, Eq. (6) is satisfied by energies $E_N = E_X - E_b$ greater than the direct gap, corresponding to resonant impurity states.

Let us now briefly recall the basic aspects of the resolvent operator formalism, which is very helpful in investigating the optical properties of these states. Let H be the Hamiltonian of our problem,

$$H = H_0 + V, \tag{7}$$

where H_0 is unperturbed crystal Hamiltonian, whose eigenstates are the Bloch functions, and V is the impurity potential. We introduce the resolvent $G(\hbar\omega)$, formally related to H by

$$G(\hbar\omega) = 1/(\hbar\omega - H + i\epsilon), \quad \epsilon \to 0^+, \tag{8}$$

as well as the "free" resolvent $G_0(\hbar\omega)$, corresponding to the unperturbed Hamiltonian H_0,

$$G_0(\hbar\omega) = 1/(\hbar\omega - H_0 + i\epsilon). \tag{9}$$

If $|\vec{k}\rangle$ denotes a Bloch state of the conduction band, G_0 is obviously diagonal and

$$\langle \vec{k}|G_0(\hbar\omega)|\vec{k}\rangle = 1/[\hbar\omega - E_c(\vec{k}) + i\epsilon]. \tag{10}$$

G is related to G_0 by the Dyson equation

$$G = G_0 + G_0VG, \tag{11}$$

and, of course, is not diagonal, because V does not conserve crystal momentum. However, G is diagonal in the complete set of the eigenstates, $|f\rangle$, of H, and

$$\langle f|G(\hbar\omega)|f\rangle = 1/(\hbar\omega - E_f + i\epsilon). \tag{12}$$

It follows easily from these definitions that the (normalized) density of states, in presence of the impurity, is given by

$$\rho(\hbar\omega) \equiv \frac{1}{N}\sum_f \delta(\hbar\omega - E_f) = -\frac{1}{\pi N}\mathrm{Im}\sum_f \langle f|G(\hbar\omega)|f\rangle$$

$$= -\frac{1}{\pi N}\mathrm{Im}[\mathrm{Tr}G(\hbar\omega)], \tag{13}$$

and since the trace does not depend on the representation, we may as well write

$$\rho(\hbar\omega) = -\frac{1}{\pi N}\mathrm{Im}\sum_{\vec{k}} \langle \vec{k}|G(\hbar\omega)|\vec{k}\rangle, \tag{14}$$

involving only the matrix elements of G between conduction Bloch states. Accordingly, the unperturbed density of states is

$$\rho_0(\hbar\omega) = -\frac{1}{\pi N}\mathrm{Im}[\mathrm{Tr}G_0(\hbar\omega)]$$

$$\equiv -\frac{1}{\pi N}\mathrm{Im}\sum_{\vec{k}} \langle \vec{k}|G_0(\hbar\omega)|\vec{k}\rangle. \tag{15}$$

Note that if we restrict the summation in Eq. (14) to a given region of the Brillouin zone, e.g., the one surrounding the Γ point in the model adopted here, we obtain

$$-\frac{1}{\pi N}\mathrm{Im}\sum_{\vec{k}}^{\Gamma} \langle \vec{k}|G(\hbar\omega)|\vec{k}\rangle = \frac{1}{N}\sum_{\vec{k}}^{\Gamma}\sum_f |\langle \vec{k}|f\rangle|^2\delta(\hbar\omega - E_f), \tag{16}$$

i.e., a density of states weighted according to the admixture of Bloch functions near the center of the zone in each state. This quantity will be referred to as the spectral weight of the region Γ in the following. Finally, a simple formula for the optical-absorption coefficient in the one-electron approximation is obtained by assuming a simple nondegenerate valence band and constant momentum matrix elements between valence and conduction band states. Apart from constant prefactors, if we denote by $|v\vec{k}\rangle$ a valence-band Bloch state of energy $-E_v(\vec{k})$, we obtain

$$\alpha(\hbar\omega) = \frac{1}{\omega^2}\sum_{\vec{k},f} |\langle v\vec{k}|p|f\rangle|^2 \delta(\hbar\omega - E_f - E_v(\vec{k})),$$

and after some formal manipulations,

$$\alpha(\hbar\omega) = -\frac{1}{\pi\omega^2}\sum_{\vec{k}} |\langle v\vec{k}|p|\vec{k}\rangle|^2 \,\mathrm{Im}\langle\vec{k}|G(\hbar\omega - E_v(\vec{k}))|\vec{k}\rangle$$

$$\simeq -\frac{1}{\pi\omega^2}|p_{cv}|^2 \,\mathrm{Im}\sum_{\vec{k}}\langle\vec{k}|G(\hbar\omega - E_v(\vec{k}))|\vec{k}\rangle. \tag{17}$$

This formula will be somewhat modified in Sec. IV, to include excitonic effects. It is easy to recognize in Eq. (17) the joint density of states of conduction and valence bands, if G is replaced by G_0.

Our problem now will be to obtain the matrix elements of G between Bloch states and to evaluate the traces appearing in the expressions for the quantities of interest here, Eq. (13)–(17).

III. OPTICAL PROPERTIES IN THE ONE-ELECTRON APPROXIMATION

In this section we will investigate the optical properties of resonant states neglecting electron-hole interaction effects. We will therefore consider optical transitions involving free holes and resonant electron states.

Let us first suppose to have only one impurity in the host alloy, deferring until later the discussion of the dependence of our results on the impurity concentration. When the Koster-Slater potential matrix elements, Eq. (5) are inserted into Eq. (11), written in the Bloch representation, the latter becomes

$$\langle\vec{k}|G(\hbar\omega)|\vec{k}'\rangle = \langle\vec{k}|G_0(\hbar\omega)|\vec{k}\rangle\delta_{\vec{k}\vec{k}'} + \sum_{\vec{q}}\langle\vec{k}|G_0(\hbar\omega)|\vec{k}\rangle U_0\langle\vec{q}|G(\hbar\omega)|\vec{k}'\rangle, \tag{18}$$

which is easily solved to give

$$\langle\vec{k}|G|\vec{k}'\rangle = \langle\vec{k}|G_0|\vec{k}\rangle\delta_{\vec{k}\vec{k}'} + \langle\vec{k}|G_0|\vec{k}\rangle\langle\vec{k}'|G_0|\vec{k}'\rangle U_0\Big/\Big(1 - U_0\sum_{\vec{q}}\langle\vec{q}|G_0|\vec{q}\rangle\Big). \tag{19}$$

Equation (19) expresses G in terms of G_0, whose matrix elements are given in Eq. (10). In the denominator of the second term, the trace of G_0 appears, whose imaginary part is related to the unperturbed density of states (DOS) and whose real part is (P denotes the Cauchy principal value)

$$\mathrm{Re}\sum_{\vec{k}}\langle\vec{k}|G_0(\hbar\omega)|\vec{k}\rangle = P\sum_{\vec{k}}\frac{1}{\hbar\omega - E_c(\vec{k})} = NP\int\frac{\rho_0(E)}{\hbar\omega - E}dE, \tag{20}$$

where $\rho_0(E)$ is the unperturbed DOS normalized to 1, given in our model by a summation of terms of the form given in Eq. (2). Therefore one easily obtains[6,7]

$$U_0\sum_{\vec{k}}\langle\vec{k}|G_0(\hbar\omega)|\vec{k}\rangle = V_0[R(\hbar\omega) - i\pi\rho_0(\hbar\omega)] \equiv V_0\sum_i[R_i(\hbar\omega) - i\pi\rho_{0i}(\hbar\omega)], \tag{21}$$

with

$$R_i(E) = \pi C_i\{(E - E_i - \Delta_i) + [(E - E_i)(E - E_i - 2\Delta_i)]^{1/2} \times[\Theta(E_i - E) - \Theta(E - E_i - 2\Delta_i)]\}, \tag{22}$$

so that all terms on the right-hand side of Eq. (19) have simple analytical expressions. It is important to notice the resonant character of the denominator of the second term, whose real part vanishes at the resonance energy. However, $\rho_0(\hbar\omega) \neq 0$ for $\hbar\omega > E_\Gamma$, and the corresponding peak in $G(\hbar\omega)$ has a finite width, corresponding to the autoionization lifetime. We now insert Eq. (19) into the expression of the DOS, Eq. (13) (which we normalize to 1), to obtain

$$\rho(\hbar\omega) = \rho_0(\hbar\omega) - \frac{1}{\pi N}\mathrm{Im}\Bigg(\sum_{\vec{k}}[\langle\vec{k}|G_0(\hbar\omega)|\vec{k}\rangle]^2 \times\frac{U_0}{1 - V_0[R(\hbar\omega) - i\pi\rho_0(\hbar\omega)]}\Bigg). \tag{23}$$

The DOS splits therefore into two terms, the first being the host crystal DOS, and the second being the "extra" DOS associated with the impurity.[10] The latter term is readily evaluated by observing that

$$\frac{1}{N}\sum_{\vec{k}}[\langle\vec{k}|G_0(\hbar\omega)|\vec{k}\rangle]^2 = \int\frac{\rho_0(E)}{(\hbar\omega - E + i\epsilon)^2}dE = -\frac{d}{d(\hbar\omega)}[R(\hbar\omega) - i\pi\rho_0(\hbar\omega)], \tag{24}$$

so that Eq. (23) allows to obtain the extra DOS associated with one nitrogen impurity, which is of

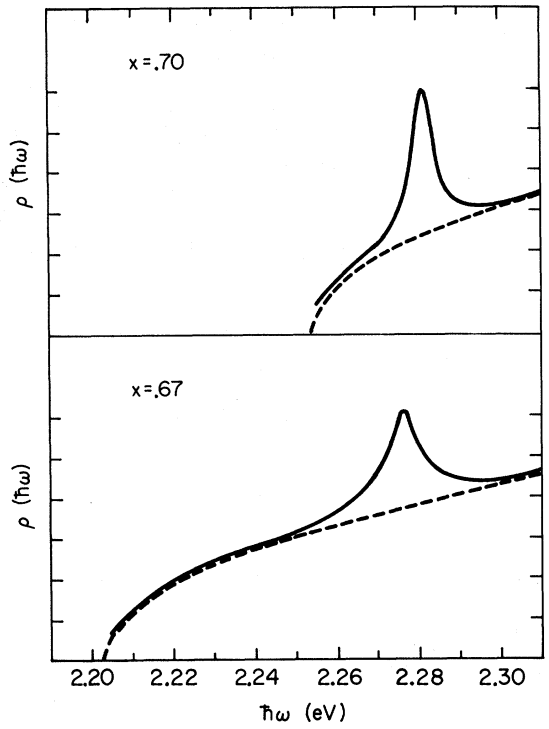

FIG. 3. Computed density of states ρ (in arbitrary units) vs energy (solid line) for $In_{1-x}Ga_xP$:N, with $n_N = 10^{18}$ cm^{-3}. Top panel: $x = 0.70$; bottom panel: $x = 0.67$. The dashed line is the N-free conduction-band density of states.

course a quantity of order $1/N$. If we can assume that the Bloch waves are scattered independently by each impurity, the extra DOS is linear in the concentration, and we obtain

$$\rho(\hbar\omega) = \rho_0(\hbar\omega) - n_N \Omega V_0 \frac{R'(\hbar\omega) V_0 \rho_0(\hbar\omega) + \rho_0'(\hbar\omega)[1 - V_0 R(\hbar\omega)]}{[1 - V_0 R(\hbar\omega)]^2 + \pi^2 V_0^2 \rho_0^2(\hbar\omega)}, \quad (25)$$

where n_N is the concentration of nitrogen impurities, and Ω is the volume of the unit cell.

The range of validity of this approximation, which neglects all interference between different scattering centers can be established by recalling that, if the resonance energy is E_N, the wavelength of the resonantly scattered Bloch states is $\sim 1/k_0$, with $E_c(\vec{k}_0) = E_N$. Therefore, if the average separation $\bar{r}$ between two impurities is much greater than $1/k_0$, all interference effects are negligible. The above condition depends on the concentration of the nitrogen impurities, which determines $\bar{r}$, on the composition of the alloy, which determines E_N, and on the Γ minimum effective mass, which determines the wave vector k_0. Inserting reasonable values of the effective mass for the alloys of interest here, we find that for $n_N \sim 10^{18}$ cm^{-3} the approximation is valid for alloy compositions such that $E_N - E_\Gamma \gtrsim 5$–10 meV. It is important to remark that when the resonance is too close to the band minimum, not only is the linearity in concentration untenable, but the one-site Koster-Slater potential is no longer adequate in a situation in which interferences depending on the details of the phase shifts are significant. This is evident from the inability of this model to provide reasonable results for nitrogen-pair bound states.[24]

In Fig. 3, the density of states, as computed from Eq. (25), is plotted for $In_{1-x}Ga_xP$:N for $x = 0.70$ and $x = 0.67$, and $n_N = 10^{18}$ cm^{-3}. The presence of the impurity results in a sharp, resonant structure above the conduction band minimum. In Fig. 4, the spectral weight of the region surrounding Γ is plotted, which is obtained by considering only the contribution of R_Γ and $\rho_{0\Gamma}$ to Eq. (24), and which is more closely related to the optical absorption and emission spectra. Note that no sharp structure is present for $n_N = 10^{18}$ and that, for $n_N = 10^{19}$, on the high-energy side of the resonance, a pronounced decrease appear. A comparison with Fig. 3 clearly indicates that the states contributing to the resonance peak have large admixtures of X and L minima Bloch functions, and that the admixture of functions with $\vec{k} \sim 0$, which are the only ones contributing to optical matrix elements, is further reduced for $\hbar\omega > E_N$.

It is interesting to remark that an integrable singularity $\sim(\hbar\omega - E_\Gamma)^{-1/2}$ appears near the threshold, and is due to the presence of $R'(\hbar\omega)$ and

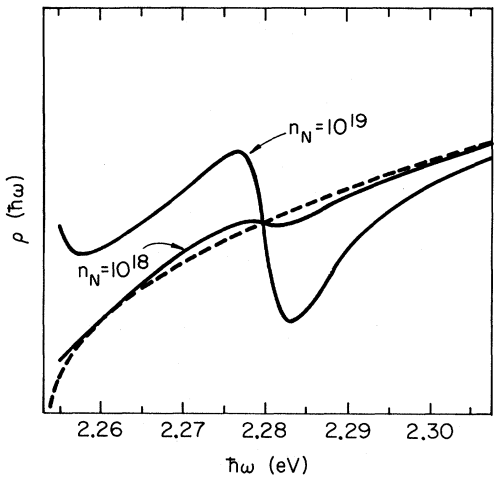

FIG. 4. Spectral weight of the Γ region (in arbitrary units) in $In_{1-x}Ga_xP$:N, $x = 0.70$ and $n_N = 10^{18}$ or $n_N = 10^{19}$ cm^{-3} (solid line); the dashed line is the N-free conduction-band density of states.

$\rho_0'(\hbar\omega)$ in Eq. (25). This threshold singularity is however of small area and would be smeared out by any inhomogeneous broadening mechanism present in real systems; furthermore, in the optical absorption, that we will consider next, the shape of the threshold will be greatly affected by the electron-hole Coulomb interaction.

Let us now turn our attention to the evaluation of the optical absorption coefficient, Eq. (17), in which, in contrast to the formula for the spectral weight of Γ, Eq. (16), the dispersion of the valence band states appears, leading to a further broadening of the impurity-induced structure. When Eq. (19) is used,

$$\langle\vec{k}|G(\hbar\omega-E_v(\vec{k}))|\vec{k}\rangle=\langle\vec{k}|G_0(\hbar\omega-E_v(\vec{k}))|\vec{k}\rangle+[\langle\vec{k}|G_0(\hbar\omega-E_v(\vec{k}))|\vec{k}\rangle]^2U_0\Big/\Big(1-U_0\sum_{\vec{q}}\langle\vec{q}|G_0(\hbar\omega-E_v(\vec{k}))|\vec{q}\rangle\Big), \tag{26}$$

so that it is readily seen that the expression for the absorption coefficient splits into a term identical to the absorption in the absence of the impurities and an "extra" absorption due to the presence of the impurities. The quantity to evaluate is therefore

$$\Delta\alpha=-\frac{1}{\pi N}\,\mathrm{Im}\left[\sum_{\vec{k}}\left(\frac{1}{\hbar\omega-E_v(\vec{k})-E_c(\vec{k})+i\epsilon}\right)^2\frac{V_0}{1-V_0[R(\hbar\omega-E_v(\vec{k}))-i\pi\rho_0(\hbar\omega-E_v(\vec{k}))]}\right]. \tag{27}$$

Contributions to the imaginary part can be split into two terms:

$$\Delta\alpha=-\frac{1}{\pi N}\,\mathrm{Im}\sum_{\vec{k}}\left(\frac{1}{\hbar\omega-E_{cv}(\vec{k})+i\epsilon}\right)^2\frac{V_0[1-V_0R(\hbar\omega-E_v(\vec{k}))]}{[1-V_0R(\hbar\omega-E_v(\vec{k}))]^2+\pi^2V_0^2\rho_0^2(\hbar\omega-E_v(\vec{k}))}$$

$$+\frac{1}{N}\,\mathrm{Re}\sum_{\vec{k}}\left(\frac{1}{\hbar\omega-E_{cv}(\vec{k})+i\epsilon}\right)^2\frac{V_0^2\rho_0(\hbar\omega-E_v(\vec{k}))}{[1-V_0R(\hbar\omega-E_v(\vec{k}))]^2+\pi^2V_0^2\rho_0^2(\hbar\omega-E_v(\vec{k}))}, \tag{28}$$

where $E_{cv}(\vec{k})$ stands for $E_c(\vec{k})+E_v(\vec{k})$. Contributions to the first term arise only from $\vec{k}$ such that $\hbar\omega=E_{cv}(\vec{k})$ and to the second term only from $\vec{k}$ such that $\hbar\omega-E_v(\vec{k})>E_\Gamma$. Therefore, in the region of interest here, that is for $E_\Gamma<\hbar\omega<E_X$ (or E_L), all the contribution is from wave vectors close to the Γ point, as it was to be expected. In this limited region, one can assume

$$E_c(\vec{k})=E_\Gamma+\alpha_c k^2,\quad E_v(\vec{k})=\alpha_v k^2, \tag{29}$$

and proceed to an evaluation of Eq. (28). To carry out the integration, use is made of the identity

$$\int\left(\frac{1}{\hbar\omega-E+i\epsilon}\right)^2 f(E,\hbar\omega)\,dE$$

$$=-\frac{d}{d(\hbar\omega)}\int\frac{1}{\hbar\omega-E+i\epsilon}f(E,\hbar\omega)\,dE$$

$$+\int\frac{1}{\hbar\omega-E+i\epsilon}\frac{\partial}{\partial(\hbar\omega)}f(E,\hbar\omega)\,dE, \tag{30}$$

so that the calculation is eventually reduced to the evaluation of some principal value integrals which can be computed with lengthy but straightforward procedures.

Numerical results are shown in Fig. 5, computed with parameters corresponding to $In_{1-x}Ga_xP$, with $x=0.70$. In order to make the impurity-induced

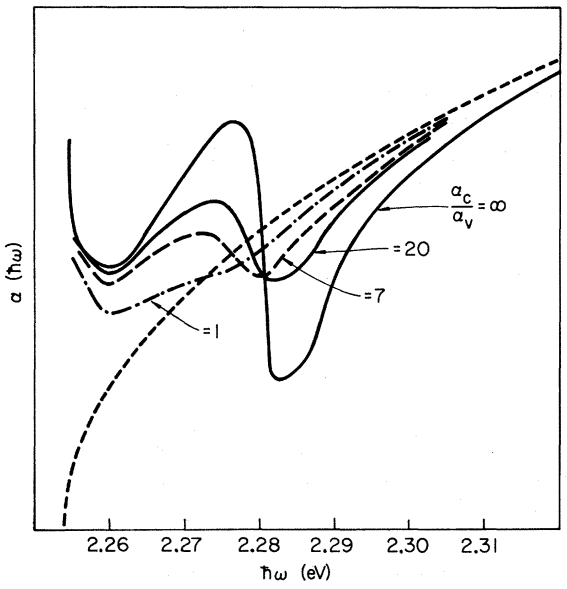

FIG. 5. Line shape of optical absorption in $In_{1-x}Ga_xP$:N, $x=0.70$, $n_N=10^{19}$ for several values of the ratio of the hole to the electron mass α_c/α_v. The line shapes are scaled so that the N-free parabolic interband edge (dashed line) is the same for all values of α_c/α_v. For $\alpha_c/\alpha_v\to\infty$, the line shape becomes identical to Fig. 4. All curves are computed ignoring any effect of the electron-hole Coulomb interaction.

structure discernible, we consider a high concentration, $n_N \sim 10^{19}$ cm^{-3}. The ordinate scale is arbitrary, and the results are scaled in such a way that the unperturbed absorption square root threshold is the same for all values of the hole to the electron mass ratio α_c/α_v. As this ratio becomes larger and larger, we recover the line shape of Fig. 4, which coincides, apart from a constant factor, with the absorption in the limit of a completely flat valence band.

Totally similar results are obtained for $GaAs_{1-x}P_x$, with compositions in the neighborhood of $x \sim 0.40$. The main qualitative feature of these curves is a broad resonance-antiresonance profile, which is rapidly smeared out by the dispersion of the valence bands. It is understood that this calculation is not intended to aim at a detailed quantitative comparison with experiment, because too many simplifications concerning the structure of the valence bands and the nature of recombination processes have been introduced, but we believe that this line shape, characteristic of interference between the discrete state and the continuum of band states, is not introduced by our approximations. This behavior will be discussed in more detail, after showing that it is still present when several features of the calculated spectrum are modified by the effect of excitonic interactions.

IV. OPTICAL PROPERTIES OF RESONANT EXCITONS

It is well known[1,3] that the nitrogen impurity in GaP is capable of binding an exciton, by trapping an electron in the short-range isoelectronic potential and then binding a hole in the resulting Coulomb field. An approximate form of the bound exciton wave function is obtained[24] by considering the product of a Koster-Slater state for the electron and a hydrogenic 1s wave function for the hole. In this section, this picture is included in our description of resonant states in N-doped semiconductor alloys, and we will consider the optical properties of virtually bound excitons autoionizing into the continuum of electron-hole pairs near Γ. In the following, the same model description of the host crystal is used, but, in order to keep the calculations within manageable limits, some reasonable approximations have to be introduced.

We start by redefining the zeroth-order or unperturbed description of the system. For reasons that will soon be clear, we include part of the potential V, acting on electrons, in H_0, and then consider the remaining part as the interaction Hamiltonian. More precisely, we include in the new H_0 the projection of V in the X and L regions of the Brillouin zone, and consider as interaction Hamiltonian the part of V connecting the X and L region states with states near Γ, and the states of the region Γ with one another. Furthermore, in contrast to the theory of Sec. III, we must include valence states explicitly in our description of the states of the system.

If we denote with $|\vec{k}_e \vec{k}_h\rangle$ the state in which an electron is present in the conduction band, with crystal momentum $\vec{k}_e$, and one, with momentum $\vec{k}_h$, is missing from the valence band, the free resolvent G_0 can be split into $G_{0\Gamma}$, with matrix elements only between states with $\vec{k}_e$ in the Γ region

$$\langle \vec{k}_e \vec{k}_h | G_{0\Gamma}(\hbar\omega) | \vec{k}_e' \vec{k}_h' \rangle = \delta_{\vec{k}_e \vec{k}_e'} \delta_{\vec{k}_h \vec{k}_h'} \times 1/[\hbar\omega - E_c(\vec{k}_e) - E_v(\vec{k}_h) + i\epsilon], \tag{31}$$

and G_{0A}, with matrix elements between states with $\vec{k}_e$ in the X and L regions and which we assume to be given by

$$\langle \vec{k}_e \vec{k}_h | G_{0A}(\hbar\omega) | \vec{k}_e' \vec{k}_h' \rangle = \langle \vec{k}_e \vec{k}_h | a \rangle [1/(\hbar\omega - E_a + i\epsilon)] \langle a | \vec{k}_e' \vec{k}_h' \rangle , \tag{32}$$

with

$$\langle \vec{k}_e \vec{k}_h | a \rangle = \frac{C}{E_b - E_c(\vec{k}_e)} \frac{(8 a_0^3/\pi)^{1/2}}{(1 + a_0^2 k_h^2)^2} . \tag{33}$$

In Eqs. (31) and (32), $|a\rangle$ is the bound exciton state described before, and obtained as the product of an electron bound in a Koster-Slater potential with energy E_b, and of a hydrogenic hole wave function with effective Bohr radius a_0 and binding energy $E_b - E_a$. C is a normalization constant. By the assumption equation (32), we completely neglect the continuum states of the X and L regions and retain only the (virtually) bound state which is pulled out of these conduction-band minima by the part of the potential included in the zeroth-order Hamiltonian. This approximation retains therefore the dominant part of the interaction, which is the scattering of virtually bound electrons into the Γ continuum, and neglects the scattering of electrons between the X-L and the Γ continuum states, which plays a minor role in the optical properties in the range defined by $\hbar\omega < E_X$ or E_L. It is also important to recall that the density of states of the conduction band at X and L is much larger[6,7] than at Γ, a fact which is essential to the existence of resonant states, and which will be useful in the following. Finally, it is important to note that we neglect the Coulomb interactions of holes with electrons in the Γ minimum, as we are interested only in the optical properties above the threshold region.

Our problem now is to determine the effect of

turning on the part of the impurity potential that acts on the Γ conduction band states. We must solve the Dyson equation for $G(\hbar\omega)$, Eq. (11). Once the matrix elements of G are known, the optical absorption coefficient can be obtained from a formula similar to Eq. (17) but explicitly including the hole states

$$\alpha(\hbar\omega) = -\frac{1}{\pi\omega^2}|p_{cv}|^2 \mathrm{Im}\sum_{\vec{k},\vec{k}'}\langle\vec{k}\vec{k}|G(\hbar\omega)|\vec{k}'\vec{k}'\rangle . \tag{34}$$

Owing to the presence of factors $(1+a_0^2k^2)^{-2}$, the summation over $\vec{k}$ and $\vec{k}'$ in Eq. (34) can be limited to wave vectors near the center of the zone. It is then convenient, in analogy with Eqs. (31)–(32) to isolate the part of $G(\hbar\omega)$ which has matrix elements between states in which the electrons are in the Γ region, which will be referred to as $G_\Gamma(\hbar\omega)$. Analogously, it will prove convenient to denote by $G_{A\Gamma}$ the part having matrix elements between states with electrons in the X or L and Γ regions, respectively. Equation (11) then becomes a system

$$\begin{aligned} G_\Gamma &= G_{0\Gamma} + G_{0\Gamma}VG_{A\Gamma} + G_{0\Gamma}VG_\Gamma , \\ G_{A\Gamma} &= G_{0A}VG_\Gamma . \end{aligned} \tag{35}$$

Taking matrix elements and recalling that

$$\langle\vec{k}_e\vec{k}_h|V|\vec{k}'_e\vec{k}'_h\rangle = U_0\delta_{\vec{k}_h\vec{k}'_h}, \tag{36}$$

Equation (35) becomes

$$\begin{aligned} \langle\vec{k}_e\vec{k}_h|G_\Gamma|\vec{k}'_e\vec{k}'_h\rangle &= \delta_{\vec{k}_e\vec{k}'_e}\delta_{\vec{k}_h\vec{k}'_h}\langle\vec{k}_e\vec{k}_h|G_{0\Gamma}|\vec{k}_e\vec{k}_h\rangle + \langle\vec{k}_e\vec{k}_h|G_{0\Gamma}|\vec{k}_e\vec{k}_h\rangle U_0 \\ &\times\left(\sum_{\vec{k}''_e}^{A}\langle\vec{k}''_e\vec{k}_h|G_{A\Gamma}|\vec{k}'_e\vec{k}'_h\rangle + \sum_{\vec{k}''_e}^{\Gamma}\langle\vec{k}''_e\vec{k}_h|G_\Gamma|\vec{k}'_e\vec{k}'_h\rangle\right), \\ \langle\vec{k}_e\vec{k}_h|G_{A\Gamma}|\vec{k}'_e\vec{k}'_h\rangle &= \sum_{\vec{k}'''_e}^{A}\sum_{\vec{k}''_h}\langle\vec{k}_e\vec{k}_h|G_{0A}|\vec{k}''_e\vec{k}''_h\rangle U_0\sum_{\vec{k}'''_e}^{\Gamma}\langle\vec{k}'''_e\vec{k}''_h|G_\Gamma|\vec{k}'_e\vec{k}'_h\rangle . \end{aligned} \tag{35'}$$

If we now sum the latter equation over $\vec{k}_e$, and substitute the summation in the former, we obtain [with the help of Eq. (41)]

$$\begin{aligned} \langle\vec{k}_e\vec{k}_h|G_\Gamma|\vec{k}'_e\vec{k}'_h\rangle &= \delta_{\vec{k}_e\vec{k}'_e}\delta_{\vec{k}_h\vec{k}'_h}\langle\vec{k}_e\vec{k}_h|G_{0\Gamma}|\vec{k}'_e\vec{k}'_h\rangle + \frac{8a_0^3C^2}{\pi}\langle\vec{k}_e\vec{k}_h|G_{0\Gamma}|\vec{k}_e\vec{k}_h\rangle \\ &\times\frac{1}{\hbar\omega - E_a + i\epsilon}\frac{1}{(1+a_0^2k_h^2)^2}g(\vec{k}'_e,\vec{k}'_h) + \langle\vec{k}_e\vec{k}_h|G_{0\Gamma}|\vec{k}_e\vec{k}_h\rangle U_0\sum_{\vec{k}''_e}^{\Gamma}\langle\vec{k}''_e\vec{k}_h|G_\Gamma|\vec{k}'_e\vec{k}'_h\rangle , \end{aligned} \tag{37}$$

where we have introduced the function

$$g(\vec{k}'_e,\vec{k}'_h) = \sum_{\vec{k}_e}^{\Gamma}\sum_{\vec{k}_h}\frac{1}{(1+a_0^2k_h^2)^2}\langle\vec{k}_e\vec{k}_h|G_\Gamma|\vec{k}'_e\vec{k}'_h\rangle . \tag{38}$$

Summing both sides of Eq. (37) over $\vec{k}_e$, the summation over $\vec{k}''_e$ in the right-hand side can be expressed in terms of $g(\vec{k}'_e\vec{k}'_h)$ and of known quantities. Furthermore, multiplying Eq. (37) by $(1+a_0^2k_h^2)^{-2}$ and summing over $\vec{k}_e$ and $\vec{k}_h$, $g(\vec{k}'_e,\vec{k}'_h)$ is completely expressed in terms of known quantities and we finally obtain

$$\begin{aligned} \langle\vec{k}_e\vec{k}_h|G_\Gamma|\vec{k}'_e\vec{k}'_h\rangle &= \delta_{\vec{k}_e\vec{k}'_e}\delta_{\vec{k}_h\vec{k}'_h}\langle\vec{k}_e\vec{k}_h|G_{0\Gamma}|\vec{k}_e\vec{k}_h\rangle + \delta_{\vec{k}_h\vec{k}'_h}\frac{\langle\vec{k}_e\vec{k}_h|G_{0\Gamma}|\vec{k}_e\vec{k}_h\rangle U_0\langle\vec{k}'_e\vec{k}'_h|G_{0\Gamma}|\vec{k}'_e\vec{k}'_h\rangle}{1 - V_0\Lambda_\Gamma(\hbar\omega - E_v(\vec{k}_h))} \\ &+\frac{8a_0^3C^2}{\pi}\left[\hbar\omega - E_a - \frac{8a_0^3C^2}{\pi}\sum_{\vec{q}}\left(\frac{1}{(1+a_0^2q^2)^4}\frac{\Lambda_\Gamma(\hbar\omega - E_v(\vec{q}))}{1 - V_0\Lambda_\Gamma(\hbar\omega - E_v(\vec{q}))}\right)\right]^{-1} \\ &\times\frac{\langle\vec{k}_e\vec{k}_h|G_{0\Gamma}|\vec{k}_e\vec{k}_h\rangle\langle\vec{k}'_e\vec{k}'_h|G_{0\Gamma}|\vec{k}'_e\vec{k}'_h\rangle}{[1 - V_0\Lambda_\Gamma(\hbar\omega - E_v(\vec{k}_h))][1 - V_0\Lambda_\Gamma(\hbar\omega - E_v(\vec{k}'_h))](1+a_0^2k_h^2)^2(1+a_0^2k_h'^2)^2} , \end{aligned} \tag{39}$$

which represents the solution to the Dyson equation. In Eq. (39), we have defined

$$\Lambda_\Gamma(E) = R_\Gamma(E) - i\pi\rho_{0\Gamma}(E) , \tag{40}$$

in analogy with Eq. (21), and we have taken advantage of the identity

$$V_0\Lambda_A(E_b) = 1 , \tag{41}$$

with $\Lambda_A(E_b) = R_X(E_b) + R_L(E_b)$, $\Lambda_A(E_b)$ being real because $E_b < E_X$ and E_L. Equation (41) is just the

equation for the binding energy in the Koster-Slater model.

Comparing Eq. (39) with Eq. (19), it is interesting to point out that the first two terms on the right-hand side of Eq. (39) are identical to Eq. (19), if the summation over $\vec{q}$ is restricted to the Γ region of the Brillouin zone. They therefore correspond to the effect of the impurity potential within the Γ region, ignoring the effect of the virtually bound exciton at energy E_a. The latter is accounted for in the third term, containing an energy denominator which is resonant at an energy that is shifted from the original "bare" energy E_a, because of the interaction with the Γ continuum. The imaginary part of the $\vec{q}$ summation corresponds to the finite width of the autoionizing state. Note also that $V_0\Lambda_\Gamma \ll 1$ in the region of interest here, owing to the small density of states in the Γ region, so that the other denominators in Eq. (39) do not give rise to resonant behavior.

We must now put $\vec{k}_e = \vec{k}_h \equiv \vec{k}$, $\vec{k}_e' = \vec{k}_h' \equiv \vec{k}'$ into Eq. (39) and perform the summation over $\vec{k}$ and $\vec{k}'$ to obtain the line shape of the optical-absorption coefficient, according to Eq. (34). In this summation, the first term on the right-hand side of Eq. (39) will simply reproduce the usual square-root threshold line shape of impurity-free absorption. The second term, in agreement with the above discussion, will give rise to a nonresonant, small contribution, except for the integrable threshold singularity discussed in Sec. III. The most important and structure-rich contribution comes from the last term, and is given, apart from constant prefactors, by

$$-\mathrm{Im}\left[\frac{1}{\hbar\omega - E_a - (8a_0^3C^2/\pi)S(\hbar\omega)} \times\left(\sum_{\vec{k}} \frac{\langle \vec{k}\vec{k}|G_{0\Gamma}(\hbar\omega)|\vec{k}\vec{k}\rangle}{[1 - V_0\Lambda_\Gamma(\hbar\omega - E_v(\vec{k}))](1+a_0^2k^2)^2}\right)^2\right], \tag{42}$$

where

$$S(\hbar\omega) = \sum_{\vec{q}} \frac{1}{(1+a_0^2q^2)^4} \frac{\Lambda_\Gamma(\hbar\omega - E_v(\vec{q}))}{1 - V_0\Lambda_\Gamma(\hbar\omega - E_v(\vec{q}))} \simeq \sum_{\vec{q}} \frac{1}{(1+a_0^2q^2)^4}\Lambda_\Gamma(\hbar\omega - E_v(\vec{q})). \tag{43}$$

The contribution in Eq. (42) therefore has the following structure:

$$-\mathrm{Im}\left(\frac{1}{\epsilon + ib}(c - id)^2\right) = \frac{b(c^2 - d^2) + 2\epsilon cd}{\epsilon^2 + b^2}, \tag{44}$$

and, in order to obtain expressions for a, b, c, and d as functions of ω, we assume the simple parabolic behavior, Eq. (29), near the band edges, and take advantage of the smallness of $V_0\Lambda_\Gamma$ with respect to 1. We then obtain

$$\epsilon = \hbar\omega - E_a - \pi C^2 C_\Gamma\left[\pi\left(\hbar\omega - E_\Gamma - \Delta_\Gamma - \frac{\alpha_v}{a_0^2}\right) - 16\left(\frac{a_0^2}{\alpha_v}\right)^{3/2}\int_{\hbar\omega - E_\Gamma}^{\infty} \frac{E^{1/2}(E + E_\Gamma - \hbar\omega)^{1/2}(E + E_\Gamma + 2\Delta_\Gamma - \hbar\omega)^{1/2}}{[1 + (a_0^2/\alpha_v)E]^4} dE\right], \tag{45}$$

$$b = 16\pi C^2 C_\Gamma\left(\frac{a_0^2}{\alpha_v}\right)^{3/2}\int_0^{\hbar\omega - E_\Gamma} \frac{E^{1/2}(\hbar\omega - E - E_\Gamma)^{1/2}(E + E_\Gamma + 2\Delta_\Gamma - \hbar\omega)^{1/2}}{[1 + (a_0^2/\alpha_v)E]^4} dE, \tag{46}$$

$$c = \tfrac{1}{2}\pi[(\alpha_c + \alpha_v)/a_0^2]^{3/2}[\hbar\omega - E_\Gamma - (\alpha_c + \alpha_v)/a_0^2]/[\hbar\omega + E_\Gamma + (\alpha_c + \alpha_v)/a_0^2]^2, \tag{47}$$

$$d = \pi(\hbar\omega - E_\Gamma)^{1/2}\{1 + [a_0^2/(\alpha_c + \alpha_v)](\hbar\omega - E_\Gamma)\}^{-2} \tag{48}$$

[to lowest order in $V_0 \max(\Lambda_\Gamma) \sim 10^{-2}$]. It is important to point out that in Eq. (45), the upper integration limit can be put, for numerical purposes, ~0.1 eV above the lower limit, because α_v/a_0^2 ~0.01 eV, for reasonable values of the valence-band mass and $a_0 \sim 40$ Å.

The basic features of the absorption line shape can be understood by a qualitative discussion of Eqs. (44)–(48). We first of all note that the resonance location $\hbar\omega_r$ is determined by the condition $\epsilon = 0$, and is, as expected, shifted from the "bare" value E_a. The asymmetric character of the line shape is a consequence of the change of sign of $2\epsilon cd$ on opposite sides of the resonant energy. In fact, when $\hbar\omega \sim E_\Gamma$, i.e., at the absorption threshold, both ϵ and c are negative; then they change sign at the resonance and at $\hbar\omega_c = E_\Gamma + (\alpha_c + \alpha_v)/a_0^2$, respectively. Therefore, $2\epsilon cd$ is positive near threshold, then becomes negative in the region between the two energies mentioned before, and eventually positive again beyond the larger of $\hbar\omega_r$, $\hbar\omega_c$. For the cases of interest here, $\hbar\omega_r < \hbar\omega_c$, the latter being 30 meV or more above E_Γ and the extra absorption becomes again positive at energies where ϵ is fairly large so that the positive enhancement is very small.

If we compare Eqs. (44)–(48) with the asymmetric Fano line shape,[25] we note that the two are very

similar, the only important difference being that c, which plays a role similar to Fano's parameter[25] q, varies considerably with energy over the range of interest, although it is negative (corresponding to enhancement of absorption on the low-energy side and suppression on the high-energy side) over most of it.

Numerical results, which illustrate this analysis, are shown in Figs. 6 and 7 for $GaAs_{1-x}P_x$ and $In_{1-x}Ga_xP$, for realistic values of the parameters. As can be seen by comparing Figs. 6 and 7 with Fig. 5, the inclusion of the Coulomb interaction produces considerable sharpening of the structure (note that in Figs. 6 and 7, $n_N = 10^{18}$ cm^{-3}), but preserves the resonance-antiresonance line shape, which is of fundamental nature. An emission spectrum, obtained by convoluting the absorption spectrum with the Fermi factor, is shown in Fig. 8.

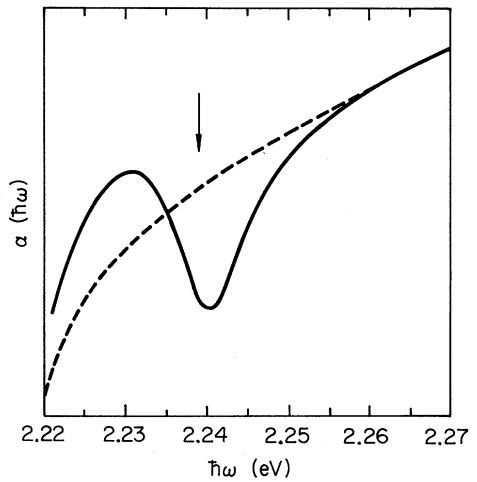

FIG. 7. Same as Fig. 6, for $In_{1-x}Ga_xP$:N, $x = 0.68$, $n_N = 10^{18}$ cm^{-3} and $\alpha_c/\alpha_v = 1$.

V. SUMMARY AND CONCLUSIONS

The main results of the present work can be summarized as follows: (i) The resolvent operator formalism has been shown to be most conveniently applicable to investigate the nature and properties of the resonant impurity states which have been observed, for a particular range of compositions, in the N-doped semiconductor alloys $GaAs_{1-x}P_x$ and $In_{1-x}Ga_xP$. (ii) While the density of states exhibits a sharp resonant peak in correspondence of the resonant state energy, when the optical absorption is computed, in a model not including excitonic effects, only a broad Fano interference profile is observed. (iii) We have succeeded in including excitonic effects in our calculation, extending therefore to semiconductor al-

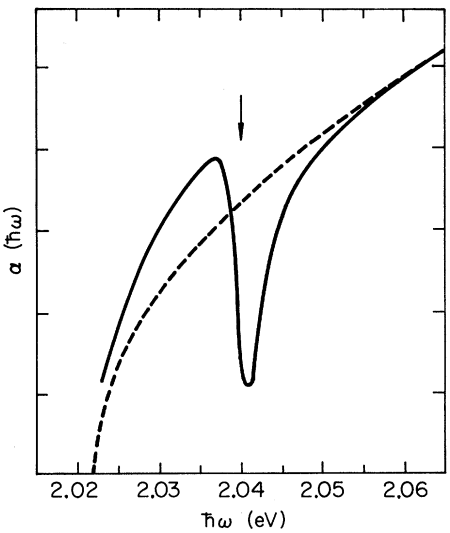

FIG. 6. Line shape of optical absorption in $GaAs_{1-x}P_x$:N, for $x = 0.41$ and $n_N = 10^{18}$ cm^{-3} (solid line). It is assumed that $\alpha_c/\alpha_v = 2$. The arrow indicates the resonance position, $\epsilon = 0$, and the dashed line is the N-free parabolic interband edge. The absorption line shape is computed including the effect of the electron-hole interaction.

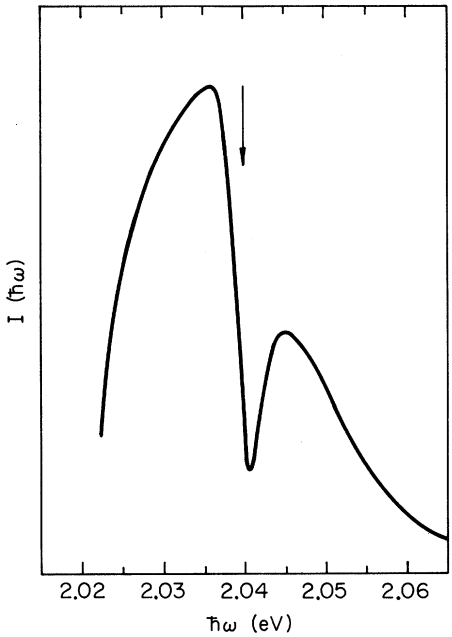

FIG. 8. Line shape of emission from $GaAs_{1-x}P_x$:N, $x = 0.41$, $n_N = 10^{18}$ cm^{-3} and $\alpha_c/\alpha_v = 2$, computed by convoluting the absorption line shape with the Fermi statistical factor corresponding to an electron temperature of 77 °K and a Fermi level 22 meV above the conduction-band minimum.

loys the picture of excitons bound (in our case, virtually bound) to isoelectronic impurities, which is successful in explaining the properties of GaP:N. The computed optical spectra confirm the Fano interference profile, which is expected, on fundamental quantum theoretical grounds, whenever a discrete state is degenerate with and coupled into a continuum of states.

Let us now briefly discuss the experimental implications of these results. It is important to notice immediately that the recombination phenomena in actual light-emitting devices are considerably more complicated than the ideal processes described in this paper, and that many effects, such as doping, transitions involving donors and acceptors, the random fields induced by compensation, donor banding at high concentration, etc., probably prevent a direct quantitative comparison of theory and experiment. On the other hand, it is certainly true that all these effects, neglected here, provide further broadening of the observed structure, and do not work in favor of the sharp, resonantly enhanced peak predicted in Refs. 7 and 12.

Nevertheless, experimental results support the present view, which is successful in understanding the quenching, rather than enhancing, effect of N traps on the laser action in $GaAs_{1-x}P_x$, and the effect of the resonant state on the effective index of refraction dispersion.[19]

By effective index we mean the quantity $n - \lambda dn/d\lambda$. This quantity is related to the spacing of the laser modes which are observed experimentally, and, on the other hand, is easily computed by a Kramers-Kronig transformation and differentiation of the absorption line shapes obtained in Sec. IV. If we subtract the unperturbed crystal absorption line shape, which will result in a smooth, increasing background in the effective index curve,[19] and consider only the "extra" absorption $\Delta\alpha$ due to the impurities, we then isolate the impurity contribution to the effective index, because of the linearity of the Kramers-Kronig relations. The resulting line shape is shown in Fig. 9, and was obtained from the computed absorption line shape shown in Fig. 6. The peak amplitude of this effective index modulation is proportional to the magnitude of the extra absorption $\Delta\alpha$, and is of order unity for $\Delta\alpha \sim -10^3\ \mathrm{cm}^{-1}$ at the antiresonance dip. The dominating feature is the sharp and very narrow positive peak, which is observed experimentally.[19] The broader negative structure on the low-energy side, on the other hand, is more likely to be smeared out by broadening and not detectable experimentally. An absorption line shape with a narrow resonantly enhanced positive peak,[7,12] would result of course in a sharp negative structure in the effective index, and is therefore difficult to reconcile with the experimental observations of Ref. 19. It is interesting to notice that the derivative term makes the overwhelming contribution to the effective index, i.e., $\lambda d\Delta n/d\lambda \gg \Delta n$. This consideration suggests that derivative techniques may be most useful in observing the resonant state, and in particular modulated absorption measurements.

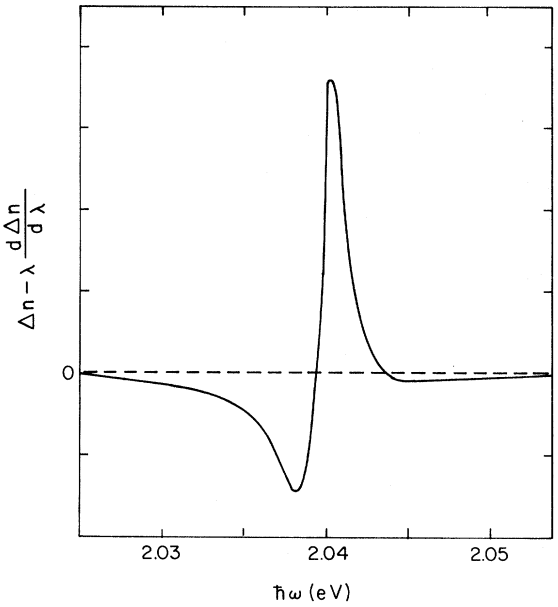

FIG. 9. Impurity contribution to the effective index of refraction $\Delta n - \lambda\, d\Delta n/d\lambda$, for $GaAs_{1-x}P_x$ with $x = 0.41$ and $\alpha_c/\alpha_v = 2$.

Finally, we wish to point out that further theoretical work is needed to understand the behavior of the optical properties in the region in which E_N is within a few meV from E_Γ, where our formulation is invalid and cooperative effects, involving pairs and larger clusters of impurities are probably important. More experimental work is also called for in this region, although, in actual samples, it may be difficult, owing to the presence of donor tails, to identify the onset of the continuum spectrum and to draw a sharp distinction between a bound and a resonant exciton region.

ACKNOWLEDGMENTS

The author is greatly indebted to Professor J. Bardeen, Professor N. Holonyak, Jr., and Professor A. B. Kunz for many invaluable discussions.

*Work supported by the U. S. Army Research Office, Durham, North Carolina under Contract No. ARO DA-HC04-74-C0005.

[1]For recent reviews of the subject, see P. J. Dean, J. Luminesc. 1, 398 (1970); W. Czaja, in *Advances in Solid State Physics*, edited by O. Madelung (Vieweg, Braunschweig, 1971), Vol. 11, p. 65.

[2]D. G. Thomas, J. J. Hopfield, and C. J. Frosch, Phys. Rev. Lett. 15, 857 (1965).

[3]D. G. Thomas and J. J. Hopfield, Phys. Rev. 150, 680 (1966).

[4]P. J. Dean and R. A. Faulkner, Appl. Phys. Lett. 14, 210 (1969).

[5]W. O. Groves, A. H. Herzog, and M. G. Craford, Appl. Phys. Lett. 19, 254 (1971).

[6]D. R. Scifres, N. Holonyak, Jr., C. B. Duke, G. G. Kleiman, A. B. Kunz, M. G. Craford, W. O. Groves, and A. H. Herzog, Phys. Rev. Lett. 27, 191 (1971).

[7]D. R. Scifres, H. M. Macksey, N. Holonyak, Jr., R. D. Dupuis, G. W. Zack, C. B. Duke, G. G. Kleiman, and A. B. Kunz, Phys. Rev. B 5, 2206 (1972).

[8]H. M. Macksey, N. Holonyak, Jr., R. D. Dupuis, J. C. Campbell, and G. W. Zack, J. Appl. Phys. 44, 1333 (1973).

[9]J. C. Campbell, N. Holonyak, Jr., A. B. Kunz, and M. G. Craford, Appl. Phys. Lett. 25, 44 (1974).

[10]J. Callaway, J. Math. Phys. 5, 783 (1964).

[11]F. Bassani, G. Iadonisi, and B. Preziosi, Phys. Rev. 186, 735 (1969).

[12]C. B. Duke, D. L. Smith, G. G. Kleiman, H. M. Macksey, N. Holonyak, Jr., R. D. Dupuis, and J. C. Campbell, J. Appl. Phys. 43, 5134 (1972).

[13]J. C. Campbell, N. Holonyak, Jr., A. B. Kunz, and M. G. Craford, Phys. Rev. B 9, 4314 (1974).

[14]J. C. Campbell, N. Holonyak, Jr., M. H. Lee, and A. B. Kunz, Phys. Rev. B 10, 1755 (1974).

[15]U. Fano, Phys. Rev. 124, 1866 (1961); U. Fano and J. W. Cooper, Rev. Mod. Phys. 40, 441 (1968).

[16]See for example, K. P. Jain, Phys. Rev. 139, A544 (1965); Y. Onodera, Phys. Rev. B 4, 2751 (1971).

[17]For effects due to the electron-phonon interaction, see J. J. Hopfield, P. J. Dean, and D. G. Thomas, Phys. Rev. 158, 748 (1967); F. Cerdeira, T. A. Fjeldly, and M. Cardona, Phys. Rev. B 8, 4734 (1973).

[18]J. J. Coleman, N. Holonyak, Jr., A. B. Kunz, W. O. Groves, D. L. Keune, and M. G. Craford, Solid State Commun. 16, 319 (1975).

[19]J. J. Coleman, N. Holonyak, Jr., M. J. Ludowise, A. B. Kunz, M. Altarelli, W. O. Groves, and D. L. Keune, Phys. Rev. Lett. 33, 1566 (1974).

[20]J. R. Klauder, Ann. Phys. (N.Y.) 14, 43 (1961).

[21]J. Hermanson, Phys. Rev. 166, 893 (1968).

[22]M. G. Craford, R. W. Shaw, A. H. Herzog, and W. O. Groves, J. Appl. Phys. 43, 4075 (1972).

[23]M. H. Lee, N. Holonyak, Jr., W. R. Hitchens, J. C. Campbell, and M. Altarelli, Solid State Commun. 15, 981 (1974); M. Altarelli, *ibid.* 15, 1607 (1974).

[24]R. A. Faulkner, Phys. Rev. 175, 991 (1968).

[25]See Eq. (20) in U. Fano, Ref. 15.